UNIVERSITY OF CALIFORNIA

Santa Barbara

Light-Activated Delivery of Proteins Using Hollow Gold Nanoshells: Protein Tracking using DLCPT (Direct Live Cell Protein Tracking)

A thesis submitted in satisfaction of the requirements for the degree Master of Science in Chemistry

by

Nicholas William Davis

Committee in charge:

Professor Norbert O. Reich

Professor Peter Ford

Professor Mahdi Abu-Omar, Chair

Professor Arnab Mukherjee

March 2023

The thesis of Nicholas William Davis is approved.

Arnab Mukherjee

Mahdi Abu-Omar, Committee Chair

Peter Ford

Norbert Reich

March 2023

ACKNOWLEDGEMENTS

The research conducted for this thesis was only a possibility thanks to the collaboration and help of many people. I would like to firstly thank Dr. Norbert Reich for his continued support through my time in his lab and as my master's advisor. His unwavering support and dedication to the project helped to push me through the many hurdles I faced along the way. I'd like to thank all of the undergraduate researchers that I've had the opportunity to work with over the years, and especially those that helped me with experiments related to my master's thesis, including Erik Sargis and Ryan Watanabe. I also wanted to thank all of the graduate researchers that I've worked in some capacity with, including Erin, Morgan, Jonathan Sandoval, Hanson Huang, Camilo Guzman, Ethan Ward, and Olivia Konttinen. Lastly, I wanted to thank all of my friends and family that have been by my side all these years with their love and support. I would like to especially thank my girlfriend, Emily, and my cat, Chester, for their constant support and love through the ups and downs of this project.

VITA OF NICHOLAS WILLIAM DAVIS

March 2023

EDUCATION

Master of Science in Chemistry, Department of Chemistry and Biochemistry, University of California, Santa Barbara, USA, March 2023

Bachelor of Science in Engineering Chemistry, Oakland University, MI, May 2017

PROFESSIONAL EMPLOYMENT

Graduate Student Researcher with Dr. Norbert Reich — 01/2019 – 12/2022

University of California, Santa Barbara

Teaching Assistance, Department of Chemistry — 09/2017 – 09/2022

General Chemistry and Organic Laboratory

University of California, Santa Barbara

Undergraduate Student Researcher with Dr. Nessan Kerrigan — 09/2015 – 09/2017

Oakland University

PUBLICATIONS

- Mondal, M.; Panda, M.; Davis, N.; McKee, V.; Kerrigan, N. Asymmetric synthesis of cyclopentanones through dual Lewis acid-catalysed [3+2]-cycloaddition of donor–acceptor cyclopropanes with ketenes. Chemical Communications 2019, 55(90), 13558-13561.

ABSTRACT

Light Activated Delivery of Proteins Using Hollow Gold Nanoshells: Protein Tracking using DLCPT (Direct Live Cell Protein Tracking)

by

Nicholas William Davis

Size and charge of proteins can hinder the intracellular delivery of biomolecules. Larger biomolecules, like proteins and peptides, have fewer delivery methods than those available for genetic material, which have a number of different delivery methods. This often limits the delivery of these larger biomolecules to viral transfections of the desired genetic material, but these can lead to gene editing of non-desired targets, due to the extended expression of the protein within cells. We've created and studied a delivery method into cells using proteins and peptides of various sizes and charges with poly-histidine tags for light-controlled delivery with hollow gold nanoshells (HGNs). The design of our delivery system includes a thiolated linker that is attached to the gold's surface and that has a nitrilotriacetic acid (NTA), biotin, or carboxylic acid (COOH) functional group on the end with polyethylene glycol (PEG) in between. Through copper-NTA affinity or 1-ethyl-3-(-3-dimethylaminopropyl) carbodiimide (EDC) chemistry, a histidine-tagged peptide or protein of interest is coupled to the HGN. Cell-penetrating peptides (CPP) on an orthogonal linker are used to accomplish endosomal uptake of the HGN. After irradiation with a pulsed femtosecond laser with non-damaging near-infrared light (NIR), endosomal disruption and protein release is accomplished. This thesis covers the construction and visualization of protein constructs using live and fixed cell imaging with DLCPT (Direct Live Cell Protein Tracking).

TABLE OF CONTENTS

LIST OF FIGURES

I. INTRODUCTION

A. FLUORESCENT PROTEIN TRACKING

Fluorescence microscopy has brought massive changes for cell biology in the visualization and tracking of proteins and peptides[1]. Many methods rely on cell fixation or specific reagents, which form the basis for antibody-based approaches, but these methods don't work for all proteins[2,3]. Fluorescent proteins as fusion proteins worked to improve the tracking of proteins in live cells, as there have been an increase in the number of different colors and variants over the years[3-6]. This increase leads to more applications being able to use the FP fusion tags for bioimaging and protein tracking. However, protein localization, stability, function, and trafficking can be adversely affected between the protein of interest and any proteins it interacts with because FPs can be larger than the protein that they are tagging[7,8]. Newer methods have arisen that utilize smaller peptide epitopes as an alternative to the larger-sized FP[9]. These methods are still limited in the ability of them to conduct live cell imaging, since they often require fixation, incubation with antibodies, association with tagged proteins or peptides, and cellular permeabilization.

The results shown in this thesis enable the tracking of proteins that are not inherently fluorescent, in live cells without gene fusions. The conjugation of organic fluorophores to a protein of interest (POI) through the reaction of native lysines on the POI and organic dyes results in protein tagging. Previous work in our lab worked on protein tracking in live cells through the use of larger-sized coiled-coil constructs[10]. The coiled-coil protein tagging approach involves a peptide fusion to a protein of interest by endogenous expression, which is tracked through another, fluorescent peptide that binds to the fused peptide[11-14]. Versatile interacting peptides (VIP) constructs were used to label proteins both inside and outside of cells. These constructs (5-7 kDa) are smaller than fluorescent fusion proteins (30 kDa), but still significantly larger than using

organic fluorophores (.5-1 kDa) to directly label proteins. Previously, in order for the VIP constructs to be used with intracellular proteins of interest, the cells needed to be fixed and the membrane had to be permeabilized[11-14]. This was later expanded to include two peptides, where coil E was the fusion peptide and coil R was delivered later on with a dye conjugated to it. This new system was called VIPER and it targeted the transferrin receptors when it was internalized and visualized over the course of hours or days. This technology helped to advance the coiled-coil platform as whole, but the need for a peptide fusion and the need for delivery of a secondary peptide continued to hinder the progression to live cell imaging with even smaller fluorescent tags. We used our technology in combination with VIPER (VIPER^{Nano}) to deliver a fluorescent peptide to track proteins in live cells[10].

B. PLASMONIC NANOPARTICLES FOR PROTEIN DELIVERY

Hollow gold nanoparticles can exist in a various shapes and sizes as inorganic particles. This thesis focuses on hollow gold nanoshells because their surfaces are easy to functionalize and they have good biocompatibility[15]. Covalent bonds are formed between the gold on the surface of the particle and a sulfhydryl functional group (SH) to form a gold-thiol bond that accomplishes surface functionalization[16]. Hollow gold nanoparticles have an adjustable surface plasmon resonance (SPR), which can increase their value as a delivery mechanism. The structure, size, and shape of the hollow gold nanoparticles affect the specific wavelength of the SPR, so hollow gold nanoparticles can be adjusted to a certain wavelength. This becomes important when dealing with the NIR light that releases the cargo from the hollow gold nanoparticles, since the oscillating electromagnetic field from the light source causes an oscillation of electrons that are free to move on the gold surface of the hollow gold nanoparticles[17,18]. This oscillation reaches a maximum amplitude at the determined wavelength of the plasmon surface resonance and under the influence

of pulsed femtosecond lasers, cleaves the gold-thiol bond on the hollow gold nanoparticles. The hollow gold nanoparticles used for this thesis were able to absorb in the near infrared (NIR) region of light and were about 40 nm in diameter. Using hollow gold nanoparticles that absorb in the NIR region of light is ideal, as biological samples remain mostly unharmed by the light[19,20]. Other sources of light-controlled systems can be quite devastating to the viability of cells, since they use higher energy light in the ultraviolet region (UV) to release the proteins of interest. Even visible light, as used for delivery of GFP and other proteins can be harmful[21]. This exposure can lead to higher levels of energy that are absorbed by the cell's tissue, which makes it unsuitable for live cell work[21]. Efficient release from endosomes remains a limiting challenge for most nanoparticle delivery approaches[22]. Transactivator of transcription (TAT) is an 11-amino acid peptide (YGRKKRRQRRR), which we and others had used to achieve excellent internalization into diverse human cancer cell lines; we used this approach for the work described here[23,24]. Once hollow gold nanoparticles (HGN) are taken up by cells, they remain inside the endosome until exposure to NIR light, which releases them into the cytosol, or until they are metabolized in cells over time, in a similar process to how ionic gold and other metals are processed by cells[25].

This occurs because the oscillation of electrons on the surface of the hollow gold nanoparticles generates enough localized heating to severe the gold-thiol bond connecting the hollow gold nanoparticles to the desired cargo. The heating is able to vaporize a very small amount of water to form vapor nanobubbles that end up surrounding the hollow gold nanoparticles, while at the same time not affecting the temperature of the overall cell[26,27]. When these nanobubbles end up collapsing, the mechanical force is enough to tear the endosomal membranes, which allows for the desired cargo to flow into the cytosol of the cell, away from the endosome[28]. There is spatiotemporal control on the release of cargo, since utilizing NIR light means that only particles

that have been irradiated will release the desired cargo, while at the same time having only localized heating on the cell that does not impact the overall cell temperature or cause cell death[26-28].

C. REFERENCES

1. Sigal, Y. M.; Zhou, R.; Zhuang, X. Visualizing and Discovering Cellular Structures with Super-Resolution Microscopy. *Science* 2018, 361 (6405), 880–887.

2. Nagarkar-Jaiswal, S.; Lee, P.-T.; Campbell, M. E.; Chen, K.; Anguiano-Zarate, S.; Cantu Gutierrez, M.; Busby, T.; Lin, W.-W.; He, Y.; Schulze, K. L.; et al. A Library of MiMICs Allows Tagging of Genes and Reversible, Spatial and Temporal Knockdown of Proteins in Drosophila. *eLife* 2015, 4.

3. Wang, Y.; Shyy, J. Y.-J.; Chien, S. Fluorescence Proteins, Live-Cell Imaging, and Mechanobiology: Seeing Is Believing. *Annu. Rev. Biomed. Eng.* 2008, 10 (1), 1–38.

4. Pakhomov, A. A.; Martynov, V. I. GFP Family: Structural Insights into Spectral Tuning. *Chem. Biol.* 2008, 15 (8), 755–764.

5. Wu, B.; Piatkevich, K. D.; Lionnet, T.; Singer, R. H.; Verkhusha, V. V. Modern Fluorescent Proteins and Imaging Technologies to Study Gene Expression, Nuclear Localization, and Dynamics. *Curr. Opin. Cell Biol.* 2011, 23 (3), 310–317.

6. Frommer, W. B.; Davidson, M. W.; Campbell, R. E. Genetically Encoded Biosensors Based on Engineered Fluorescent Proteins. *Chem. Soc. Rev.* 2009, 38 (10), 2833.

7. Costantini, L. M.; Snapp, E. L. Fluorescent Proteins in Cellular Organelles: Serious Pitfalls and Some Solutions. *DNA Cell Biol.* 2013, 32 (11), 622–627.

8. Jensen, E. C. Use of Fluorescent Probes: Their Effect on Cell Biology and Limitations. *Anat. Rec. Adv. Integr. Anat. Evol. Biol.* 2012, 295 (12), 2031–2036.

9. Kanca, O.; Bellen, H. J.; Schnorrer, F. Gene Tagging Strategies To Assess Protein Expression, Localization, and Function in Drosophila. Genetics 2017, 207 (2), 389– 412.

10. Morgan, E., Doh, J., Beatty, K. and Reich, N., 2019. VIPERnano: Improved Live Cell Intracellular Protein Tracking. *ACS Applied Materials & Interfaces* 2019, 11(40), 36383-36390.

11. Kawano, K.; Yano, Y.; Omae, K.; Matsuzaki, S.; Matsuzaki, K. Stoichiometric Analysis of Oligomerization of Membrane Proteins on Living Cells Using Coiled-Coil Labeling and Spectral Imaging. *Anal. Chem.* 2013, 85 (6), 3454–3461.

12. Wang, J.; Yu, Y.; Xia, J. Short Peptide Tag for Covalent Protein Labeling Based on Coiled Coils. *Bioconjug. Chem.* 2014, 25 (1), 178–187.

13. Doh, J. K.; White, J. D.; Zane, H. K.; Chang, Y. H.; López, C. S.; Enns, C. A.; Beatty, K. E. VIPER Is a Genetically Encoded Peptide Tag for Fluorescence and Electron Microscopy. *Proc. Natl. Acad. Sci.* 2018, 115 (51), 12961–12966.

14. Zane, H. K.; Doh, J. K.; Enns, C. A.; Beatty, K. E. Versatile Interacting Peptide (VIP) Tags for Labeling Proteins with Bright Chemical Reporters. *ChemBioChem* 2017, 18 (5), 470–474.

15. Li, J.; Xue, S.; Mao, Z.-W. Nanoparticle Delivery Systems for SiRNA-Based Therapeutics. *J. Mater. Chem.* B 2016, 4 (41), 6620–6639.

16. Boisselier, E.; Astruc, D. Gold Nanoparticles in Nanomedicine: Preparations, Imaging, Diagnostics, Therapies and Toxicity. *Chem. Soc. Rev.* 2009, 38 (6), 1759.

17. Kreibig, U.; Vollmer, M. Optical Properties of Metal Clusters; 1995, 9.

18. Cobley, C. M.; Chen, J.; Cho, E. C.; Wang, L. V.; Xia, Y. Gold Nanostructures: A Class of Multifunctional Materials for Biomedical Applications. *Chem Soc Rev* 2011, 40 (1), 44–56.

19. Prevo, B.; Esakoff, S.; Mikhailovsky, A.; Zasadzinski, J. A. Scalable Routes to Gold Nanoshells with Tunable Sizes and Response to Near-Infrared Pulsed Laser Irradiation. *Small* 2008, 4, 1183–1195.

20. Weissleder, R. A Clearer Vision for in Vivo Imaging. *Nat. Biotechnol.* 2001, 19 (4), 316–317.

21. Neves-Peterson, M.; Petersen, S.; Gajula G. UV Light Effects on Proteins: From Photochemistry to Nanomedicine. *Molecular Photochemistry - Various Aspects*, 2012

22. Park, H.-J.; Shin, J.; Kim, J.; Cho, S.-W. Nonviral Delivery for Reprogramming to Pluripotency and Differentiation. *Arch. Pharm. Res.* 2014, 37 (1), 107– 119.

23. Ramsey, J. D.; Flynn, N. H. Cell-Penetrating Peptides Transport Therapeutics into Cells. *Pharmacol. Ther.* 2015, 154, 78–86.

24. Rizzuti, M.; Nizzardo, M.; Zanetta, C.; Ramirez, A.; Corti, S. Therapeutic Applications of the Cell-Penetrating HIV-1 Tat Peptide. *Drug Discov. Today* 2015, 20 (1), 76–85.

25. Balfourier, A.; Luciani, N.; Wang, G.; Lelong G.; Ersen, O.; Khelfa, A.; Alloyeau, D.; Gazeau, F.; Carn, F. Unexpected Intracellular Biodegradation and Recrystallization of

Gold Nanoparticles. *Proceedings of the National Academy of Sciences* 2019, 117 (1), 103–113.

26. Lukianova-Hleb, E. Y.; Volkov, A. N.; Lapotko, D. O. Laser Pulse Duration Is Critical For the Generation of Plasmonic Nanobubbles. *Langmuir* 2014, 30 (25), 7425–7434.

27. Lukianova-Hleb, E. Y.; Belyanin, A.; Kashinath, S.; Wu, X.; Lapotko, D. O. Plasmonic Nanobubble-Enhanced Endosomal Escape Processes for Selective and Guided 10 Intracellular Delivery of Chemotherapy to Drug-Resistant Cancer Cells. *Biomaterials* 2012, 33 (6), 1821–1826.

28. Wu, G.; Mikhailovsky, A.; Khant, H. A.; Fu, C.; Chiu, W.; Zasadzinski, J. A. Remotely Triggered Liposome Release by Near-Infrared Light Absorption via Hollow Gold Nanoshells. *J. Am. Chem. Soc.* 2008, 130 (26), 8175–8177.

III. DIRECT LIVE CELL PROTEIN TRACKING, DLCPT: IMPROVED LIVE CELL PROTEIN TRACKING

A. Abstract

Despite its broad use, tracking proteins inside of live cells has many challenges. Fluorescent fusion proteins are commonly used and have led to a number of important discoveries in cell biology, which was awarded the 2008 Nobel Prize in Chemistry in 2008 to Osamu Shimomura, Martin Chalfie, and Roger Tsien. Fusion proteins can cause problems with native protein function and they add extra steric bulk to the desired protein of study[1]. This bulk has been shown to interfere with known protein-protein interactions, leading to erroneous interpretations[1]. The use of exogenous probes, like antibodies, for tracking cellular proteins can cause problems, since they may not cross the plasma membrane. We designed a labeling and delivery platform, Direct Live Cell Protein Tracking, DLCPT, which relies on our established use of HGNs to deliver protein and nucleic acid payloads into cells when treated with a pulsed NIR laser. This method requires the indirect attachment of the protein to the HGNs and NIR light-activated protein release of the desired protein after being taken up by the cell. We demonstrated the light-activated delivery of GFP (green fluorescent protein) and dye-labeled streptavidin into live cells. This approach has the power to lessen the steric bulk of fluorescent tags attached to the protein of interest, while also giving the ability to study protein dynamics and spatial tracking in live cells.

B. Introduction

Important biological tools, such as fluorescence microscopy, have revolutionized how cell biologists can track and visualize proteins in live cells, by allowing for the interrogation of protein function and temporal and high-resolution spatial information[2]. Many of the most common methods utilize antibody-related technologies, but these often require rather specific reagents and

are typically limited to fixed, not live cells[3,4]. While fluorescent fusion proteins can be an improvement for protein tracking and live cell bioimaging over immunolabeling, the fusion constructs are generally larger than the protein that is being studied[5-8]. This size discrepancy can cause changes in protein stability, localization, function, and trafficking[9,10].

Previously, we utilized a coiled-coil construct as a labeling platform for proteins, in which a peptide is fused to the protein of interest. The peptide fusion is incubated and dimerized with a second dye-labeled peptide to track it[11-14]. These coiled-coil tags were known as VIP (versatile interacting peptide) tag, which was later updated to VIPER to include the CoilE fusion tag and the CoilR dye-labeled peptide that was delivered using hollow gold nanoparticles. This technique was used to track intracellular proteins, like histone H2B and mitochondria, in a study of tracking intracellular proteins in live cells, as well as labeling extracellular proteins[15].

VIP (~5 kDa) tags provided a smaller fusion approach than using fluorescent fusion proteins (~30 kDa), but utilizing smaller organic fluorophores (~.5 kDa) reduces the size of the fluorescent tag to a fraction of the size of either other approach. Proteins of interest are conjugated to organic fluorophores, filtered of extra organic fluorophores, and then delivered into live cells. The delivery system requires two distinct polyethylene glycol (PEG) linkers attached to the hollow gold nanoparticles to work. One PEG linker is attached to the protein of interest and the other strand is attached to the cell-penetrating peptide that allows for the hollow gold nanoparticles to be internalized[15]. HGNs get trapped in the endosome through endocytosis until irradiated with a NIR light source[15]. While endosomal entrapment can be a big problem for many nanoparticle delivery methods, we can control the release of both the hollow gold nanoparticles and the desired protein of interest from the endosome with NIR light, where the protein of interest is released at the same time from the surface of the hollow gold nanoparticles[16-18]. Continued work on this

technology will enable the ability to track proteins in live cells with less potential harm on the function, localization, stability, and trafficking.

C. Results and Discussion

Particle Design and Characterization

Previously, VIPER fluorescent tags were used to track proteins in live cells without needing to use large fluorescent protein fusions. This system was used to track both mitochondrial and histone H2B proteins, where fusion proteins would cause steric bulk around the nucleosome core. This could cause problems with function of the H2B protein, as the DNA needs to wrap around the histone proteins[15].

While the coiled-coil system led to smaller steric bulk around the protein of interest, the use of organic fluorophores as fluorescent labels leads to an even smaller amount of steric bulk around the protein of interest. These very small tags allow for a better picture of protein dynamics, since they provide minimal disruption to function, stability, localization, and trafficking[15]. Organic fluorophores have high quantum yields, a diverse range of colors and wavelengths, and high-resolution fluorescent imaging[19-21].

We previously modeled the interaction between the GFP fusion and the function of the histones[15]. The histones fused to fluorescent proteins could negatively impact the appropriate nucleosome assembly or interactions with proteins necessary for transcription; prior work with this approach ran into unanticipated issues shown in previous studies of protein dynamics using fluorescent fusion proteins[9,10,22]. The size variation of the three tags between H2B fused to a GFP, H2B fused to a coiled-coil, and H2B conjugated to an organic fluorophore is notable for the big differences, which can visually be seen in Figure II-1. H2B is half the size of the GFP, three times

the size of the coiled-coil, and thirty times the size of organic fluorophores (Figure II-1b,c,d). Our study doesn't rely on the use of FP fusions to track proteins, but FP fusions could be used to directly compare localization of our technology.

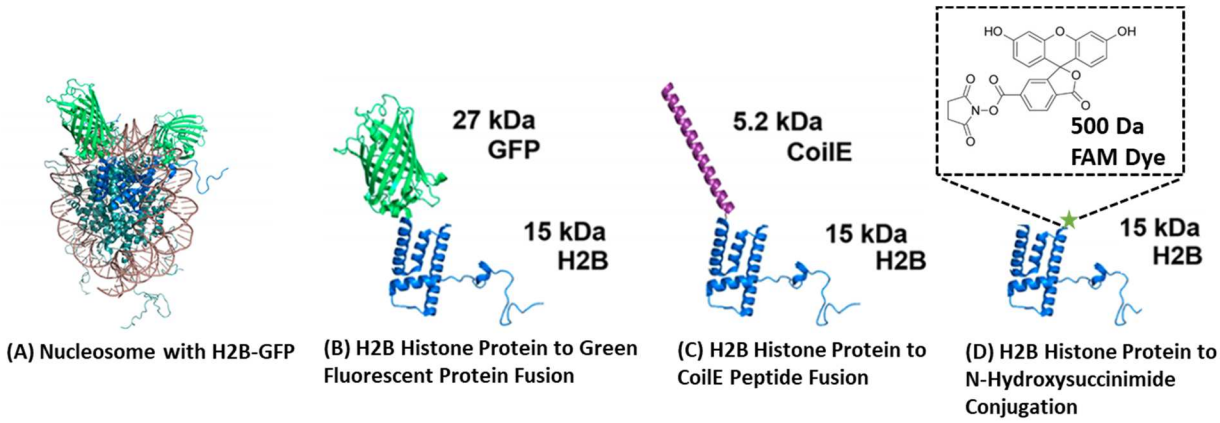

Figure II-1. FDLP relies on much smaller fluorescent protein tags. A) Nucleosome with H2B-GFP show the DNA (tan) wrapped around the octamer of histone proteins (light blue) including the two H2B proteins (dark blue) fused to GFP (green). B) H2B-GFP fusion monomer with size markers for GFP (27 kDa) and H2B (15 kDa). C) H2B-CoilE fusion monomer with size markers for CoilE (5.2 kDa) and H2B (15 kDa). D) H2B-FAM Dye conjugation with size makers for FAM Dye (.5 kDa) and H2B (15 kDa).

Previous delivery strategies utilizing HGN in our lab relied on nucleic acid linkers, rather than polyethylene glycol (PEG) linkers, to deliver siRNA, peptides, and proteins into live cells. These constructs relied on poly-histidine-tagged proteins of interest and multiple linker assembly steps, which increased the complexity and difficulty of using the approach[23-25]. There are two potential HGN functionalization strategies demonstrated in this thesis. One strategy relies on the use of 1-ethyl-3-(-3-dimethylaminopropyl) carbodiimide (EDC) and N-hydroxysuccinimide (NHS) to conjugate surface lysine with thiolated polyethylene glycol (PEG) linkers with

carboxylic acid end groups that are bound to the surface of the hollow gold nanoparticles. The other strategy relies on poly-histidine-tagged proteins in the presence of copper conjugating with thiolated PEG linkers with nitrilotriacetic acid (NTA) end groups that are bound to the surface of the hollow gold nanoparticles. Transactivator of transcription (TAT) peptides linked to biotinylated PEG strands by streptavidin allow for the internalization into cells, while second strands are attached to the protein of interest (Figure II-2a). The two strands are attached to the hollow gold nanoparticles in equal amounts to enable successful loading of both the TAT internalization peptide, as well as the protein of interest with an organic dye conjugated to it. The hollow gold nanoparticles would range in size between 40 nm without linkers and 102 nm once the protein of interest, TAT, and streptavidin were attached to the HGNs (Figure II-2c). The surface plasmon resonance (SPR) is shown to be present in the bare HGNs and maintained after the addition of PEG linkers, streptavidin, and bovine serum albumin (BSA), with the PSR declining after the addition of the biotin-TAT (Figure II-2c). A bright, green-fluorescent FAM dye was used for dye-labeling most of the proteins, including bovine serum albumin (BSA), cell cycle-regulated methyltransferase (CcrM), thymine DNA glycosylase (TDG), haemophilus parahaemolyticus type-2 restriction enzyme (HhaII), tumor suppressor (P53), DNA methyltransferase 3 alpha (3A), and DNA (cytosine-5)-methyltransferase 3-like (3L) proteins, as it is ideal for fluorescent tracking of cells (Figure II-4a).

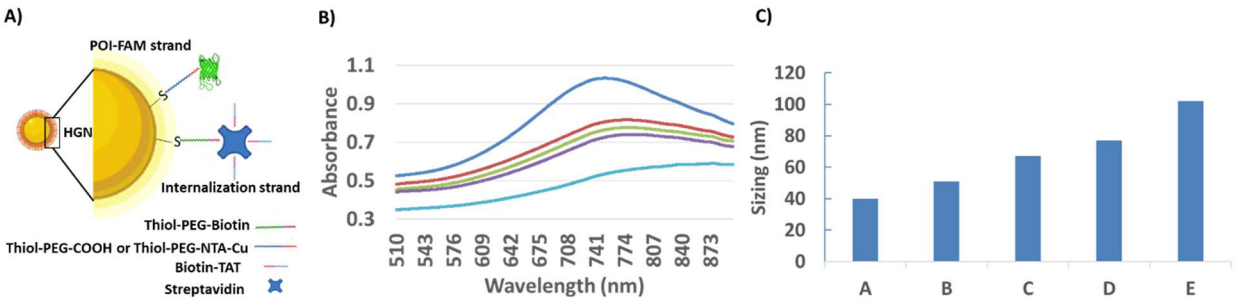

FIGURE II-2: Particle assembly strategy and characterization of HGN constructs. A) Illustration of HGN construct with 1:1 loading of Thiol-PEG-NTA (or Thiol-PEG-COOH):Thiol-PEG-Biotin, labeled POI-FAM strand and internalization strand, respectfully. The biotin terminated PEG was labeled with streptavidin TAT for internalization while the orthogonal NTA or COOH terminated strand allowed for POI-FAM loading. B) Maximum wavelength of bare HGN is 750 nm, representing the plasmon surface resonance, which allow release of cargo when irradiated with NIR 800nm light. Dark blue line is bare HGN; red line is HGN with 3K PEG COOH linker attached; green line is HGN with 1:1 3K PEG COOH:3K PEG Biotin linkers attached; purple line is HGN with BSA and streptavidin attached to 1:1 3K PEG COOH:3K PEG Biotin linkers; light blue line is HGN with BSA, streptavidin, and TAT attached to 1:1 3K PEG COOH:3K PEG Biotin. C) Size distribution of nanoparticles during coating steps. HGN (A) have a mean number dimeter of 40 nm; HGN-PEG-COOH (B), 51 nm; HGN-PEG-COOH:HGN-PEG-Biotin (C), 67 nm; HGN-PEG-COOH:HGN-PEG-Biotin with BSA and streptavidin attached (D), 77 nm; HGN-PEG-COOH:HGN-PEG-Biotin with BSA, streptavidin, and TAT attached (E), 102 nm.

Internalization

We've shown previously that both hollow gold nanoparticles without the TAT peptide for internalization and proteins by themselves are unable to passively diffuse into cells[11,26]. HeLa cells (~100,000 cells as counted by hemocytometer) were incubated with 32 pM HGN-protein-FAM dye in DMEM with 10% FBS for two hours and then imaged with both brightfield and fluorescent microscopy to confirm the internalization of the hollow gold nanoparticles. Hollow gold nanoparticle constructs appear as black spots in brightfield microscopy, while the HGN-protein-

FAM constructs appear as fluorescent spots on fluorescent microscopy, which can be seen in Figure II-2c-f. The presence of these black and fluorescent spots inside of cells show successful internalization of the hollow gold nanoparticles (Figure II-3). The internalization of the hollow gold nanoparticle constructs into human cells was controlled by the TAT peptide, which could be swapped out for other targeting peptides, depending of the desired cell application[28] (Figure II-2).

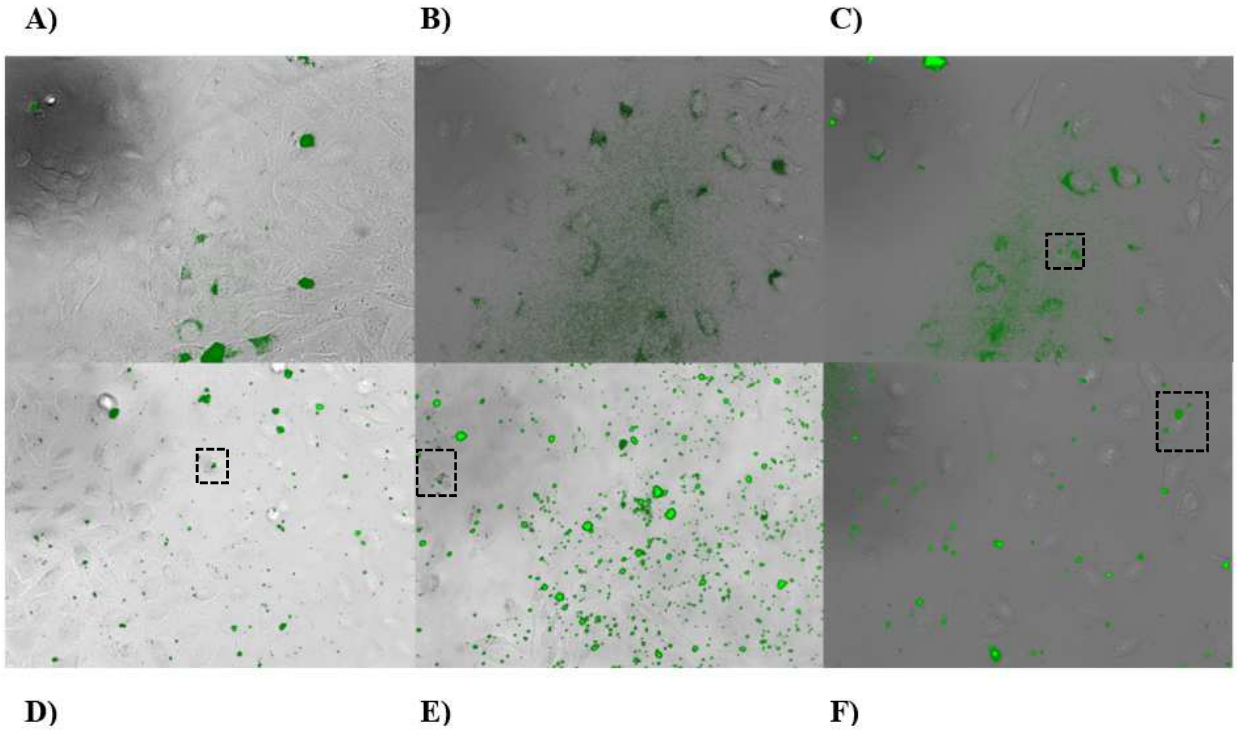

FIGURE II-3: Internalization experiment in fixed HeLa cells with fluorescence overlapped with brightfield images. Boxed cells are cells demonstrating successful internalization of HGN. A) No HGN or protein added. B) GFP added without HGN C) 1:1 HGN-PEG-COOH-TAT:HGN-PEG-FITC internalized, with colinker fluorescence for visualization of particles. D) 1:1 HGN-PEG-COOH-TAT:HGN-PEG-COOH-GFP internalized, with GFP fluorescence for visualization. E) 1:1 HGN-PEG-COOH-GFP:HGN-PEG-Strep-Biotin-TAT internalized, with GFP fluorescence for visualization. F) 1:1 HGN-

PEG-NTA-Cu-BSA-FITC:HGN-PEG-NTA-Cu-TAT internalized, with FITC dye for visualization.

Load and Release Characterization and Optimization

Endogenous tags are often used in labeling technologies, but control over how much of the desired protein of interest is released is limited[27]. By utilizing hollow gold nanoparticles to deliver FAM-labeled proteins into cells, the amount of cargo released can be controlled by the NIR laser power. There is minimal protein release observed in samples that are not irradiated with NIR light, as shown in Figure II-4c and Figure II-5, while there is an increase in the amount of desired protein release with higher laser powers (Figure II-5).

Proteins were labeled with FAM dyes with NHS groups that reacted with lysine native to the protein of interest. Proteins were stored in storage buffer and filtered multiple times using centrifugation filters with a 10K molecular weight cutoff, separating excess dye from the protein of interest. This is demonstrated in Figure II-4a, where an SDS-PAGE gel was run with various dye-labeled proteins. These proteins were compared to the initial dye to see if the protein were adequately dye-labeled and if they had removed all of the excess dye. The gel was scanned for fluorescence with a gel scanner in the green light region, which aligned with the FAM dye used.

Proteins were also observed using SDS-PAGE and a Coomassie stain to see an increase in the molecular weight of the proteins, upon addition of PEG linkers to the protein of interest via EDC chemistry (Figure II-4b). The presence of protein at a higher molecular weight after the addition demonstrates successful EDC chemistry in the two columns to the left in Figure II-4b and the presence of protein with unchanged molecular weight demonstrates that not every protein is

being modified with the added amine and carboxyl linkers, which can be seen in Figure II-4b. The ratio of dyed to undyed protein is a ratio of 1.5-2:1, as determined by ImageJ.

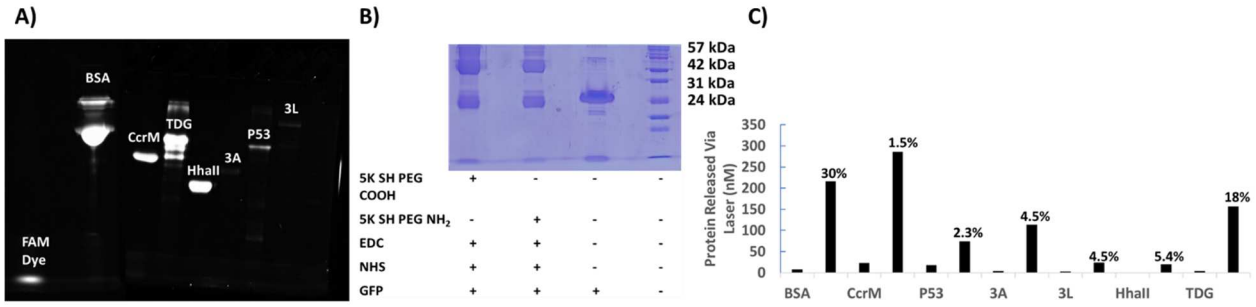

FIGURE II-4: Dye-labeling of proteins, protein attachment via EDC chemistry, and protein release with NIR light. A) Proteins were conjugated with a FAM-NHS organic dye, before excess dye was filtered away using 10K Amicon Ulta Centrifugation Filters. Proteins were then conjugated to HGN via EDC chemistry. Fluorescent FAM images were obtained from BioRad Chemidoc. B) EDC Chemistry between PEG linkers and GFP demonstrate an increase in molecular weight of GFP after the reaction, showing that the linkers attached to the GFP. SDS-PAGE gel run at 200V for 60 minutes, followed by Coomassie stain and then washed of excess stain. C) Release from NIR light demonstrates that bovine serum albumin (BSA) released the highest percent of attached protein.

By analyzing the fluorescent FAM label on the protein of interest in a cell-free setting, calculation of protein loading and release was determined. Hollow gold nanoparticles (32 pM) were incubated with 1 μM of the dye-labeled protein of interest and then washed to remove the excess dye-labeled protein of interest via centrifugation. To release the loaded protein from the surface of the hollow gold nanoparticles, a pulsed 800 nm laser at 850 mW power irradiated the HGN for 15 seconds. The hollow gold nanoparticles were pelleted by centrifugation and the supernatant was scanned with a fluorescent plate reader, Tecan Spark. The results were compared

to a known protein concentration with a known FAM fluorescence titration curve to determine the concentration of released protein. A total loading calculation of the desired protein of interest was determined by dissolving the samples that were not irradiated with NIR light with a KCN buffer to chemically release the desired protein from the HGN-protein-FAM constructs. This was utilized to find the percent release after irradiation with NIR light pulsed laser.

We managed to attach up to 6,800 proteins-FAM per particle, which was lower, but comparable to previous work[27]. Figure II-4c showed a release of protein-FAM of up to 30% only with the presence of NIR irradiation. Optimization studies utilizing bovine serum albumin (BSA) demonstrated an increase to 55% at max laser power when a 1:1 linker ratio was utilized when delivering proteins into cells. By adding more of either linker, there was a loss in the percent release of the protein of interest (Figure II-5).

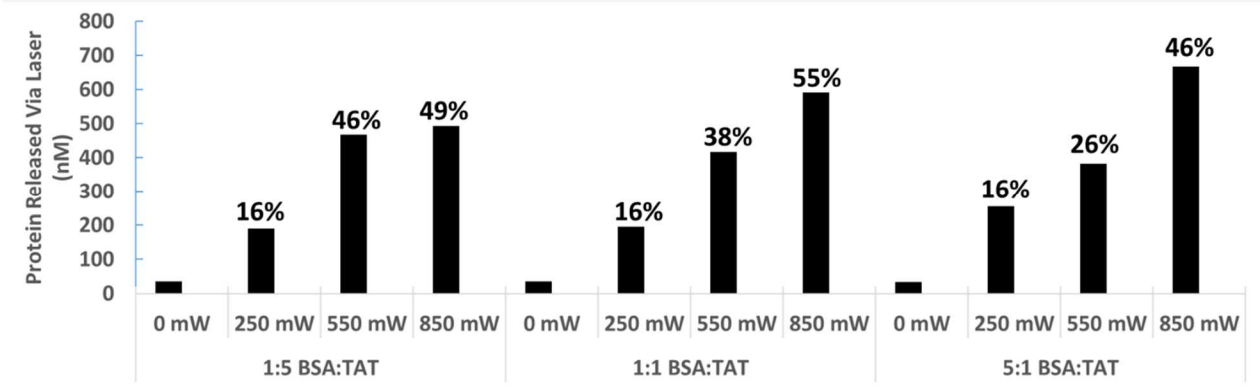

Figure II-5: Optimization of BSA Loading onto HGNs. Ratio of BSA:TAT conjugation onto HGN-PEG-COOH particles determines 1:1 particles allow for maximum release of BSA with 16 μM initial BSA concentration.

Further experiments were conducted to release dyed protein of interest from the hollow gold nanoparticles after they were internalized into live HeLa cells. The samples were irradiated with a pulsed NIR light laser that was set to 820 nm from a commercial two-photon confocal

microscope, which demonstrated the release of protein from the fluorescent puncta change before and during irradiation (Figure II-6a). Individual cells were isolated and then irradiated over 3 minutes to show the release and then photobleaching of the fluorescent protein. Individual fluorescent proteins can be seen moving inside of the cytosol of the HeLa cells (Figure II-6b). The software was able to track the movement of the fluorescent protein through analysis of green light in the selected cell after laser irradiation. The fluorescence appeared stationary in samples that were not irradiated with NIR light. Individual cells were then isolated and irradiated to form a Z-stack of the cell, which showed that the fluorescence was localized in the inner layers of the cell, rather than being stuck to the outside of the cell (Figure II-6c). We conclude that FDLPnano works in a NIR light-dependent manner for the tracking of the desired protein of interest in live cells, based on our tracking experiment.

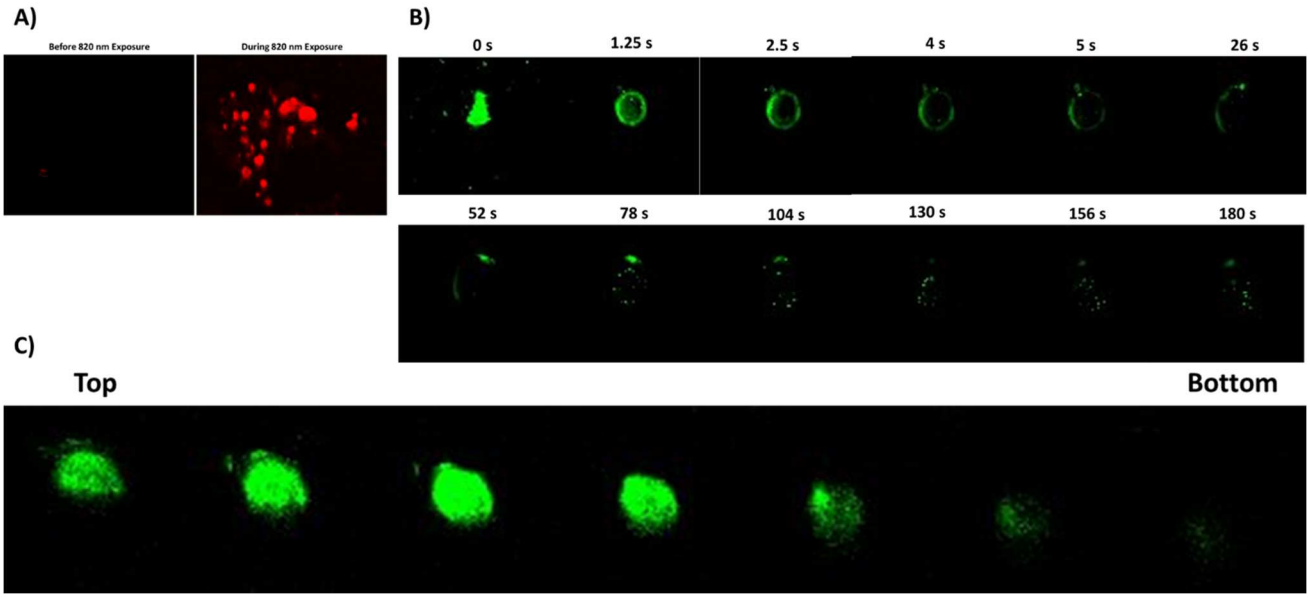

FIGURE II-6: Two photon microscope releases fluorescent proteins from HGN into live HeLa cells. A) HGN-PEG-COOH-Strep-Dye internalized and released when hit with 820 nm light, demonstrated by increase in fluorescence when particles release Strep-Dye.

B) Time-lapse images of 1:1 HGN-PEG-COOH-GFP:HGN-PEG-Streptavidin-Biotin-TAT particles releasing and then moving freely inside of a single cell. C) Z-stacks of a single cell with 1:1 HGN-PEG-COOH-GFP:HGN-PEG-Streptavidin-Biotin-TAT particles, which shows the fluorescence is internalized in the middle of the cell.

D. Conclusions

Our experiments demonstrate that the steric bulk of fluorescent tags to the protein of interest can be reduced, while at the same time, being used to study protein tracking and dynamics in live cells from the light-activated delivery and release of dye-labeled protein using hollow gold nanoparticles. The DLCPT (Direct Live Cell Protein Tracking) platform provides a method for tracking proteins without large peptide or protein fusions by utilizing small organic fluorophores that are smaller than 1 kDa in size and can be conjugated to the protein of interest. This system can utilize different cell-penetrating peptides on the hollow gold nanoparticles for the internalization into various cell lines, which makes it a widely appliable system. The usage of a RPARPAR peptide in the place of the TAT peptide would allow the hollow gold nanoparticles to internalize into PPC-1 cells that express the neuropilin-1 receptor[28]. We successfully showed temporal and spatial control of the technology when exposing hollow gold nanoparticles to NIR light, which control when the dye-labeled protein is released and how much is released.

E. Materials and Methods

HGN synthesis and characterization

Hollow gold nanoparticles were synthesized using a protocol used previously that utilizes a sacrificial silver template. These particles were dialyzed overnight at room temperature in sodium citrate buffer (500 mM) using dialysis cassettes (20 kDa MWCO). The hollow gold

nanoparticles were attached to PEG linkers to coat the surface of the particles with HS-PEG-biotin (3.4K), HS-PEG-NTA (3.4K), or HS-PEG-COOH (3.4K). Hollow gold nanoparticles were diluted in PBS and measured with a UV-Vis spectrophotometer (Shimadzu) at a wavelength from 300 nm to 900 nm to acquire absorbance spectra. The sizing was acquired from a Malvern Zetasizer Nano ZS that measured the size of the particles using dynamic light scattering.

Streptavidin and protein of interest functionalization

10μL of 1mM stock of HS-PEG-COOH (3.4K) were incubated with 10 μL of 10 mg/mL N-hydroxysuccinimide (NHS) and 10 μL of 10 mg/mL 1-ethyl-3-(-3-dimethylaminopropyl) carbodiimide (EDC) for 15 minutes at 4°C, followed by the addition of the protein of interest. This mixture was stirred at 4°C on a rocker for two hours, before 1 mL of 64 pM of HGN was added and incubated on a rocker overnight at 4°C. The particles were washed x4 with PBS with 0.01% Tween-20 (PBST) at 14,000 RPM for 10 minutes at 4°C the next day to remove excess PEG and protein of interest.

Streptavidin could be functionalized by the same method or it could be functionalized using HS-PEG-Biotin (3.4K). 100 μL of 5 mg/mL streptavidin was added to 10 μL of 1mM of HS-PEG-Biotin at 4°C and allowed to stir on a rocker for 1 hour. 1 mL of 64 pM of HGN was then added and incubated on a rocker overnight at 4°C. The next day, the particles were washed x4 with PBST at 14,000 RPM for 10 minutes at 4°C to remove excess PEG and Streptavidin. 2.5 μL of 2 mM biotin-TAT (Anaspec) was added twice, with a 30-minute incubation time at 4°C after each addition. The particles were then washed two times with PBST to remove any excess biotin-TAT.

Proteins were also functionalized using HS-PEG-NTA (3.4 K). 10 μL of 1 mM of HS-PEG-NTA (3.4 K) was incubated with 2.5 μL of 50 mM Tris(2-carboxyethyl)phosphine

hydrochloride (TCEP) for 15 minutes at room temperature on a rocker to prevent disulfide bonds from forming between linkers. 1 mL of 64 pM HGN were added and stirred on a rocker at room temperature overnight. The next day, the particles were washed x4 with PBST. 200 µL of the functionalized 32 pM particles are incubated with 20 µL of 5 mM $CuCl_2$ and 4 µL of 50 µM protein of interest at 4°C for 30 minutes. Particles were then washed x4 times to remove any excess reagents.

Calculation of dye-labeled protein load and release in cell-free environment

The protein of interest was labeled with a FAM dye for protein tracking with a N-hydroxysuccinimide dye which reacted with potential lysine residues. KCN solution [1 mM $K_3Fe(CN)_6$ and 0.1 M KCN] was incubated with 32 pM hollow gold nanoparticles to dissolve the particles and release the dye-labeled protein to calculate how much protein was loaded onto the particles[19]. A fluorescent plate reader, Tecan Spark, was used to measure the fluorescence intensity compared to the concentration of the protein-dye to calculate the concentration of the released protein by using a linear calibration curve. A femtosecond Ti:sapphire regenerative amplified (Spectraphysics Spitfire) NIR pulsed laser light running at 1 kHz irradiated the hollow gold nanoparticles that were attached to the dye-labeled proteins of interest for 15 seconds at 250 mW – 850 mW laser power. The laser power was able to be quantified utilizing a thermopile power meter. Samples were pelleted via centrifugation and separated from the supernatant that is removed and inserted into a 96 well plate. The pellet was then dissolved using KCN and FAM fluorescence was used to determine how much protein was attached to the hollow gold nanoparticles.

SDS-PAGE preparation and analysis

12% SDS-PAGE gel made with 4 mL of 30% acrylamide-bis, 2.6 mL of 1.5 M Tris-HCl at a pH of 8.7, 3.2 mL of milliQ H_2O, 50 µL of 10% ammonium persulfate (APS), 100 µL of 10% sodium dodecyl sulfate (SDS), and 8 µL tetramethylethylenediamine (TEMED). Stacking gel was added on top of the gel from 666 µL of 30% acrylamide-bis, 500 µL of 0.5M Tris-HCl at a pH of 6.8, 2.73 mL of milliQ H_2O, 40 µL of 10% SDS, 20 µL of 10% APS, and 8 µL of TEMED with 1 mm comb inserted.

Samples were added to 20 mL wells with a 1:1 mixture of 1x Laemmli buffer and protein and allowed to run at 200 V for 1 hour. FDLP imaged with BioRad Chemidoc at 488 nm to confirm dye labeling of protein and removal of excess dye. Excess dye was removed using 10K Amicon Ulta Centrifugation Filters, using storage buffer (50 mM Tris-HCl, 200 mM NaCl, 1 mM EDTA, 0.5 mM DTT, 20% Glycerol, pH 7.8) to wash the protein of interest.

Non-fluorescent gels are stained with Coomassie stain for 30 minutes at room temperature and then washed with destain (50% methanol, 40% H_2O, 10% acetic acid) multiple times to remove excess stain.

Brightfield and fluorescence microscopy for internalization analysis

HeLa cells were plated in a 6-well plate at $3x10^5$ cells per well in 1000 µL DMEM +10% FBS one day before particle internalization experiments. Hollow gold nanoparticles that were attached to dye-labeled proteins were put in DMEM + 10% FBS (32 pM) and sonicated. The particles were then added to the plated HeLa cells at 37°C and 5% CO2 for two hours. Cells were then washed with PBS x4 times and incubated with 1 mL of 4% formaldehyde for 15 minutes to fix cells. In brightfield and internalization experiments, cell fixation was used to preserve the cells for imaging. Cells were washed to remove extra formaldehyde with PBS x3 times. Samples were

observed on a Zeiss Axiovert 200 motorized inverted microscope with a bright field condenser and a 20x objective lens.

Cellular release using two-photon microscope and analysis with Image J

For release experiments inside of cells, a two-photon microscope is needed to supply the NIR light source. 100,000 HeLa cells were plated the day before two-photon use in the middle of an Ibidi μ-Dish (35 mm). Hollow gold nanoparticles were loaded with dye-labeled proteins or fluorescent proteins in the previously described method before incubation with HeLa cells. 32 pM of hollow gold nanoparticles were put in 500 μL of DMEM with 10% FBS and added to the middle of an Ibidi dish after being sonicated. The Ibidi dish was incubated at 37°C at 5% CO_2 for two hours.

Afterwards, the cells were washed with PBS four times to remove excess hollow gold nanoparticles and then 2 mL of DMEM with 10% FBS, HEPES, high glucose, and no phenol red was added to the Ibidi dish. HEPES can be an important additive for imaging experiments because it keeps the pH of the DMEM stable during the irradiation and transport of the samples. Samples were focused using a Bruker Ultima In Vitro two-photon and confocal microscope equipped with a 20x water immersion objective lens (600 μm x 600 μm) and irradiated using NIR light at 1.65 fps at 512 x 512. The Prairie Reader software turned on the NIR laser, which could be set from 690 nm – 1300 nm at different potential powers. The correct dyes were selected and an increase in voltage would result in more signal from the dye-labeled proteins. The NIR light could be set at different powers to get the optimal release of the protein of interest when the 820 nm light irradiated the cell volume. Images were collected before and during laser irradiation to confirm release of the dye-labeled and fluorescent proteins by looking at FAM and RFP fluorescence. Afterwards, ImageJ was used to analyze the images acquired.

Confocal microscopy was run with a 20x water objective lens with laser excitation sources for FAM and RFP fluorescence at 488 nm and 558 nm, respectively. Time-lapse images of FAM fluorescence were collected using the xyt function for 3 minutes. All images were falsely-colored using standard lookup tables in ImageJ: FAM (green) and RFP (red).

F. REFERENCES

1. Calabro, Viola. GFP Fusion Proteins: A Solution or a Problem? *Biomedical Journal of Scientific & Technical Research* 2018, 5 (5), 4805-4810.

2. Sigal, Y. M.; Zhou, R.; Zhuang, X. Visualizing and Discovering Cellular Structures with Super-Resolution Microscopy. *Science* 2018, 361 (6405), 880–887.

3. Jensen, E. C. Use of Fluorescent Probes: Their Effect on Cell Biology and Limitations. *Anat. Rec. Adv. Integr. Anat. Evol. Biol.* 2012, 295 (12), 2031–2036.

4. Nagarkar-Jaiswal, S.; Lee, P.-T.; Campbell, M. E.; Chen, K.; Anguiano-Zarate, S.; Cantu Gutierrez, M.; Busby, T.; Lin, W.-W.; He, Y.; Schulze, K. L.; et al. A Library of MiMICs Allows Tagging of Genes and Reversible, Spatial and Temporal Knockdown of Proteins in Drosophila. *eLife* 2015, 4.

5. Wang, Y.; Shyy, J. Y.-J.; Chien, S. Fluorescence Proteins, Live-Cell Imaging, and Mechanobiology: Seeing Is Believing. *Annu. Rev. Biomed. Eng.* 2008, 10 (1), 1–38.

6. Pakhomov, A. A.; Martynov, V. I. GFP Family: Structural Insights into Spectral Tuning. *Chem. Biol.* 2008, 15 (8), 755–764.

7. Wu, B.; Piatkevich, K. D.; Lionnet, T.; Singer, R. H.; Verkhusha, V. V. Modern Fluorescent Proteins and Imaging Technologies to Study Gene Expression, Nuclear Localization, and Dynamics. *Curr. Opin. Cell Biol.* 2011, 23 (3), 310–317.

8. Frommer, W. B.; Davidson, M. W.; Campbell, R. E. Genetically Encoded Biosensors Based on Engineered Fluorescent Proteins. *Chem. Soc. Rev.* 2009, 38 (10), 2833.

9. Costantini, L. M.; Snapp, E. L. Fluorescent Proteins in Cellular Organelles: Serious Pitfalls and Some Solutions. *DNA Cell Biol.* 2013, 32 (11), 622–627

10. Huang, L.; Pike, D.; Sleat, D. E.; Nanda, V.; Lobel, P. Potential Pitfalls and Solutions for Use of Fluorescent Fusion Proteins to Study the Lysosome. *PLoS ONE* 2014, 9 (2), e88893.

11. Zane, H. K.; Doh, J. K.; Enns, C. A.; Beatty, K. E. Versatile Interacting Peptide (VIP) Tags for Labeling Proteins with Bright Chemical Reporters. *ChemBioChem* 2017, 18 (5), 470–474.

12. Doh, J. K.; White, J. D.; Zane, H. K.; Chang, Y. H.; López, C. S.; Enns, C. A.; Beatty, K. E. VIPER Is a Genetically Encoded Peptide Tag for Fluorescence and Electron Microscopy. *Proc. Natl. Acad. Sci.* 2018, 115 (51), 12961–12966.

13. Kawano, K.; Yano, Y.; Omae, K.; Matsuzaki, S.; Matsuzaki, K. Stoichiometric Analysis of Oligomerization of Membrane Proteins on Living Cells Using Coiled-Coil Labeling and Spectral Imaging. *Anal. Chem.* 2013, 85 (6), 3454–3461.

14. Wang, J.; Yu, Y.; Xia, J. Short Peptide Tag for Covalent Protein Labeling Based on Coiled Coils. *Bioconjug. Chem.* 2014, 25 (1), 178–187.

15. 11. Morgan, E., Doh, J., Beatty, K. and Reich, N., 2019. VIPERnano: Improved Live Cell Intracellular Protein Tracking. *ACS Applied Materials & Interfaces* 2019, 11(40), 36383-36390.

16. Li, H.; Nelson, C. E.; Evans, B. C.; Duvall, C. L. Delivery of Intracellular-Acting Biologics in pro-Apoptotic Therapies. *Curr. Pharm. Des.* 2011, 17 (3), 293–319.

17. Pearce, M. C.; Gamble, J. T.; Kopparapu, P. R.; O'Donnell, E. F.; Mueller, M. J.; Jang, H. S.; Greenwood, J. A.; Satterthwait, A. C.; Tanguay, R. L.; Zhang, X.-K.; et al. Induction of Apoptosis and Suppression of Tumor Growth by Nur77-Derived Bcl-2 Converting Peptide in Chemoresistant Lung Cancer Cells. *Oncotarget* 2018, 9 (40).

18. Huang, X.; Lai, Y.; Braun, G. B.; Reich, N. O. Modularized Gold Nanocarriers for TAT-Mediated Delivery of SiRNA. *Small* 2017, 13 (8), 1602473.

19. Waggoner, A. Fluorescent labels for proteomics and genomics. *Current Opinion in Chemical Biology* 2006, 10 (1), 62-66.

20. Jensen, E. Use of Fluorescent Probes: Their Effect on Cell Biology and Limitations. *The Anatomical Record: Advances in Integrative Anatomy and Evolutionary Biology* 2012 295 (12), 2031-2036.

21. Li, B.; Yu, Q.; Duan, Y. Fluorescent labels in biosensors for pathogen detection. *Critical Reviews in Biotechnology* 2013, 35 (1), 82-93.

22. Luger, K. Nucleosomes: Structure and Function. *In Encyclopedia of Life Sciences; John Wiley & Sons, Ltd, Ed.; John Wiley & Sons, Ltd: Chichester* 2001.

23. Morales, D.; Morgan, E.; McAdams, M.; Chron, A.; Shin, J.; Zasadzinski, J.; Reich, N. Light-Triggered Genome Editing: Cre Recombinase Mediated Gene Editing with Near-Infrared Light. *Small* 2018, 14 (30), 1800543.

24. Morgan E.; Wupperfeld D.; Morales D.; Reich N. Shape Matters: Gold Nanoparticle Shape Impacts the Biological Activity of siRNA Delivery. *Bioconjugate Chem.* 2019, 30 (3), 853-860.

25. Morales D.; Wonderly W.; Huang X.; McAdams M.; Chron A.; Reich N. Affinity-Based Assembly of Peptides on Plasmonic Nanoparticles Delivered Intracellularly with Light Activated Control. *Bioconjugate Chem.* 2017, 28 (7), 1816-1820.

26. Morgan, E.; Gamble, J. T.; Pearce, M. C.; Elson, D. J.; Tanguay, R. L.; Kolluri, S. K.; Reich, N. O. Improved in Vivo Targeting of BCL-2 Phenotypic Conversion through Hollow Gold Nanoshell Delivery. *Apoptosis Int. J. Program. Cell Death* 2019.

27. Klein, A.; Hank, S.; Raulf, A.; Joest, E. F.; Tissen, F.; Heilemann, M.; Wieneke, R.; Tampé, R. Live-Cell Labeling of Endogenous Proteins with Nanometer Precision by Transduced Nanobodies. *Chem. Sci.* 2018, 9 (40), 7835–7842.

28. Teesalu, T.; Sugahara, K. N.; Kotamraju, V. R.; Ruoslahti, E. C-End Rule Peptides Mediate Neuropilin-1-Dependent Cell, Vascular, and Tissue Penetration. *Proc. Natl. Acad. Sci.* 2009, 106 (38), 16157–16162.